FUSE

Fungal Systematics and Evolution

VOLUME 5
JUNE 2020
PAGES 119–129

doi.org/10.3114/fuse.2020.05.07

Phylogenetic placement of *Paratrichaptum* and reconsideration of *Gloeophyllales*

C.-C. Chen[1], B. Cao[2], T. Hattori[3], B.-K. Cui[4], C.-Y. Chen[1], S.-H. Wu[1,5*]

[1]Department of Plant Pathology, National Chung Hsing University, Taichung 40227, Taiwan
[2]State Key Laboratory of Mycology, Institute of Microbiology, Chinese Academy of Sciences, Beijing 100101, China
[3]Forestry and Forest Products Research Institute, Tsukuba, Ibaraki 305-8687, Japan
[4]Institute of Microbiology, Beijing Forestry University, Beijing 100083, China
[5]Department of Biology, National Museum of Natural Science, Taichung 40453, Taiwan

*Corresponding author: shwu@mail.nmns.edu.tw

Key words:
brown rot
eastern and southeastern Asia
systematics
taxonomy
wood-inhabiting fungi
new taxa

Abstract: *Paratrichaptum accuratum* is a large conspicuous polypore fungus growing on dead or living angiosperm trees in subtropical-boreal areas of China, Indonesia, Japan, and Taiwan. The present study places *P. accuratum* in the family *Gloeophyllaceae* that belongs to the order *Gloeophyllales* within *Agaricomycetes* (*Basidiomycota*), based on evidence derived from morphological and ecological characteristics, and phylogenetic analyses of sequences of nuclear rDNA regions (5.8S, nuc 18S, nuc 28S) and protein-coding genes (*rpb1*, *rpb2,* and *tef1*). The analyses presented in this study also give strong support for including *Jaapia* in *Gloeophyllaceae* and *Gloeophyllales*. Thus, the names *Jaapiaceae* and *Jaapiales* are considered here as synonyms of *Gloeophyllaceae* and *Gloeophyllales*. Since *Paratrichaptum* represents the earliest diverging lineage in *Gloeophyllales*, pileate basidiocarps and brown rot appear to be ancestral states of *Gloeophyllales*. *Paratrichaptum accuratum* may represent a relic species, according to its phylogenetic position, peculiar distribution pattern and rare occurrence.

Effectively published online: 11 October 2019.

INTRODUCTION

The genus *Paratrichaptum* was described by Corner (1987) to accommodate a monotypic species, *P. accuratum*, a large conspicuous wood-inhabiting polypore fungus. This genus is characterised by a peculiar combination of morphological features. In macromorphology, it has a pileate and sessile basidiocarp that is soft-corky and spongy in the fresh condition, poroid to daedaleoid hymenophore, and brown tubes and context. Microscopically, it possesses a monomitic hyphal system, nodose-septate generative hyphae, fasciculate cystidia, and pale brown and smooth basidiospores with thin to slightly thick walls, which have a negative reaction in Melzer's reagent. Such a combination is fairly peculiar within the polypore fungi, sustaining its position as a distinct genus (Ryvarden 1991).

Paratrichaptum accuratum is hitherto known only from Asia (Ryvarden, 1991, Núñez & Ryvarden 2001) where it grows on hardwoods (Corner 1987, Núñez & Ryvarden 2001). The holotype was collected from a highland forest of Sumatra (Indonesia), 56 years before Corner's (1987) description. Recently, this species was discovered in subtropical to boreal regions of Japan (Hokkaido, Kagoshima, Nara, Yamagata) based on four specimens collected between 1989 and 1994 (Núñez & Ryvarden 2001, Hattori 2017). Núñez & Ryvarden (2001) reported this species from Taiwan based on a specimen collected in 1922.

According to MycoBank (Robert *et al.* 2005), *P. accuratum* is placed in the family *Schizoporaceae*, in the order *Hymenochaetales*. However, this placement was never examined through molecular phylogenetic analyses since sequence data related to this species are lacking. In 2017, two specimens of *Paratrichaptum accuratum* were collected during a field trip in southern Yunnan (China), which enabled us to study the higher-rank classification for this species.

To infer the placement of *Paratrichaptum accuratum* within *Agaricomycetes*, the present study conducted phylogenetic analyses based on sequences of nuc rDNA genes and three protein-coding genes. The results allowed us to discuss the limits of the orders *Gloeophyllales* and *Jaapiales*.

MATERIALS AND METHODS

Morphological studies

Voucher specimens are deposited at the herbaria of the Kunming Institute of Botany, Chinese Academy of Sciences of PRC (KUN), the Botanical Museum, University of Oslo of Norway (O), the Forestry and Forest Products Research Institute of Japan (TFM), and the National Museum of Natural Science of ROC (TNM). Abbreviations of herbaria follow those in the Index Herbariorum (http://sweetgum.nybg.org/science/ih/). Basidiocarps and the native habitat were photographed with an Olympus TG-4 or a Nikon D5300 digital camera. All microscopic characters were examined from dried specimens with a Leica DM2500 microscope. 5 % Potassium hydroxide (KOH) with 1 % phloxine was used for observation and measurement. Melzer's

Fungal Systematics and Evolution is licensed under a Creative Commons Attribution-NonCommercial-ShareAlike 4.0 International License

© 2020 Westerdijk Fungal Biodiversity Institute

reagent was used to determine amyloidity and dextrinoidity. Cotton blue (Fluka 61335) was used as a mounting medium to check cyanophily. The following abbreviations were used for basidiospore measurements: L = mean basidiospore length with standard deviation, W = mean basidiospore width with standard deviation, Q = variation in L/W ratio, n = number of measured basidiospores from each specimen.

DNA extraction, PCR amplification, and DNA sequencing

Genomic DNA was extracted from dried specimens using a Plant Genomic DNA Extraction Miniprep System (Viogene, New Taipei, Taiwan), based on manufacturer's instructions. The sample was first homogenised with the aid of liquid nitrogen and a Tissue Lyser II (Qiagen, Hilden, Germany). We used primer pairs ITS1/ITS4 for nuc rDNA ITS1-5.8S-ITS2 (nuc ITS); PNS1/NS8 for nuc 18S rDNA (nuc 18S) (White *et al*. 1990); LR0R/LR5 for D1-D2 domains of nuc 28S rDNA (nuc 28S) (Moncalvo *et al*. 2000); RPB1-Int2f/RPB1-Cr for RNA polymerase II largest subunit (*rpb1*) (Frøslev *et al*. 2005); RPB2-f5F/RPB2-b7.1R for RNA polymerase II second largest (*rpb2*) (Liu *et al*. 1999, Matheny 2005); EF1-983F/EF1-1953R for translation elongation factor 1-α (*tef1*) (Rehner & Buckley 2005). The PCR conditions to amplify ITS, nuc 18S and nuc 28S gene regions were as follows: initial denaturation at 95 °C for 5 min, followed by 40 cycles at 94 °C for 45 s, 53 °C for ITS and 50 °C for the nuc 18S and nuc 28S for 45 s and 72 °C for 45 s and a final extension of 72 °C for 10 min. The protocols for amplifying *rpb1*, *rpb2,* and *tef1* were performed as described in Chen *et al*. (2018). The PCR products were purified and sequenced by the MB Mission Biotech Company (Taipei, Taiwan). The newly obtained sequences were edited and assembled using BioEdit v. 7.2.5 (Hall 1999), and submitted to the DNA Data Bank of Japan (DDBJ) (Table 1).

Sequence alignments and phylogenetic analyses

The dataset of concatenated 5.8S+nuc 18S+nuc 28S+*rpb1*+*rpb2*+*tef1* was used to investigate the systematic position of *Paratrichaptum accuratum* among 21 recognised orders of the class *Agaricomycetes*. Since *P. accuratum* was recovered near the orders *Gloeophyllales* and *Jaapiales* based on our preliminary phylogenies, sequences from species belonging to these two orders were selected as candidate references (Binder *et al*. 2010, Garcia-Sandoval *et al*. 2011, He *et al*. 2014, Telleria *et al*. 2015). For other representative species from *Agaricomycetes*, as well as representatives of *Dacrymycetes* and *Tremellomycetes*, we consulted studies of Lutzoni *et al*. (2004), Hibbett *et al*. (2007), Matheny *et al*. (2007), Hodkinson *et al*. (2014), Sjökvist *et al*. (2014), and Zhao *et al*. (2017). *Bullera alba* and *Dioszegia antarctica*, belonging to *Tremellomycetes*, were selected as the outgroup.

All intron regions of protein-coding genes (*rpb1*, *rpb2*, and *tef1*) and non-coding nuc rDNA were omitted. Sequences of each single-gene dataset were aligned with MAFFT v. 7.409 (Katoh & Standley 2013), using the default algorithm. Poorly aligned regions were detected by GUIDANCE2 webserver (Sela *et al*. 2015), and manually adjusted with MEGA v. 7 (Kumar *et al*. 2016), when necessary. Maximum likelihood (ML) analyses were performed for each gene with RAxML-HPC BlackBox v. 8.2.10 (Stamatakis 2014) on CIPRES Science Gateway (Miller *et al*. 2010), using 500 bootstrap (BS) replicates and the default GTR+G model. A conflict between two genes was assumed to happen when a monophyletic clade was supported with BS ≥ 70 % in a single tree but was contradicted with significant support in another (Hillis & Bull 1993). Congruence among genes was visually compared. Conflict-free alignments were concatenated and subjected to subsequent analyses. Sequence alignments are deposited at TreeBASE (submission ID: S24457; www.treebase.org).

Partitioned ML and Bayesian inference (BI) analyses were carried out for the concatenated dataset, respectively, with RAxML-HPC2 v. 8.2.10 (Stamatakis 2014) and MrBayes v. 3.2.6 (Ronquist *et al*. 2012), on CIPRES Science Gateway (Miller *et al*. 2010). ML analysis was run for 1 000 bootstrap (BS) replicates with the GTR+CAT model. For BI analysis, we used the GTR+G model for 5.8S and the GTR+I+G model for nuc 18S, nuc 28S, *rpb1*, *rpb2*, and *tef1* as selected by jModeltest v. 2.1.10 (Darriba *et al*. 2012), based on the Akaike information criterion (AIC). BI analysis was conducted for four runs with four chains each for 10 M generations, sampling one tree every 1 000 generations. The first 25 % of trees were discarded as burn-in. Remaining trees were used to construct a 50 % majority-rule consensus phylogram with Bayesian posterior probabilities (PP). Tracer v. 1.7 (Rambaut *et al*. 2018) was used to confirm that the average standard deviation of split frequencies (= 0.006589) had reached an appropriate level with Effective Sampling Sizes (ESS) > 200. TreeGraph v. 2 (Stöver & Müller 2010) and Adobe Illustrator (Adobe Systems, Inc.) were used to edit and visualise resulting trees.

RESULTS

Molecular phylogeny

In this study, we generated new sequences of six genes (5.8S, nuc 18S, nuc 28S, *rpb1*, *rpb2*, *tef1*) from two specimens of *Paratrichaptum accuratum* (Table 1). The 5.8S+nuc 18S+nuc 28S+*rpb1*+*rpb2*+*tef1* dataset included 96 species and 97 sequences. The final alignment had 7 181 positions, including gaps, of which 38 % (2696/7181) were parsimony-informative. Phylograms obtained from BI and ML analyses had similar topologies, and, thus, only the ML tree with BP and PP support values is shown (Fig. 1).

In our six-gene phylogenetic analysis, three classes, *Agaricomycetes*, *Tremellomycetes* and *Dacrymycetes*, were resolved as monophyletic clades with BP = 93–100 and PP = 1. Sequences of two specimens of *Paratrichaptum accuratum* were almost identical. They, together with *Boreostereum radiatum*, formed a basal lineage in *Gloeophyllales* (Fig. 1). *Jaapia* was recovered in *Gloeophyllales* (Fig. 1), which makes *Jaapiales* a synonym of *Gloeophyllales*. Of the 20 currently recognized orders in the *Agaricomycetes*, 19 were monophyletic (*Agaricales*, *Amylocorticiales*, *Atheliales*, *Auriculariales*, *Boletales*, *Cantharellales*, *Corticiales*, *Geastrales*, *Gloeophyllales*, *Hymenochaetales*, *Hysterangiales*, *Lepidostromatales*, *Phallales*, *Polyporales*, *Russulales*, *Sebacinales*, *Stereopsidales*, *Thelephorales*, and *Trechisporales*), with BP = 81–100 and PP = 1; only *Gomphales* lacked support (Fig. 1).

© 2020 Westerdijk Fungal Biodiversity Institute

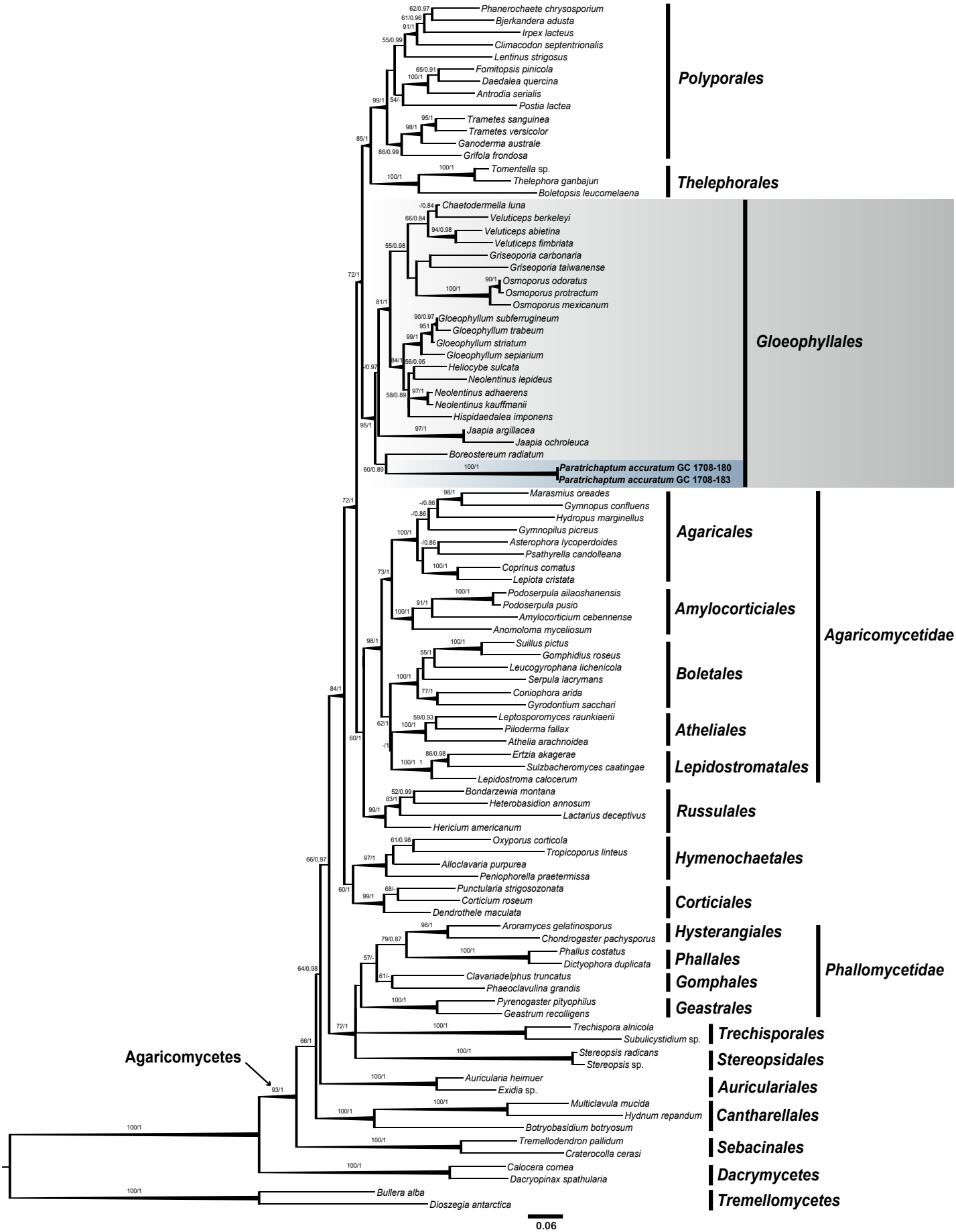

Fig. 1. Phylogenetic relationships of orders among *Agaricomycetes* inferred from 5.8S, nuc 18S, nuc 28S, *rpb1*, *rpb2,* and *tef1* sequences. Nodes are labeled with Maximum Likelihood bootstrap proportional values (BS) ≥ 50 % and Bayesian Posterior Probabilities (PP) ≥ 0.8. Thickened branches obtained supports by both BS ≥ 70 % and PP ≥ 0.95. The greyish box indicates taxa in *Gloeophyllales*. Scale bar = substitutions per site.

© 2020 Westerdijk Fungal Biodiversity Institute

Table 1. Species and sequences used in the phylogenetic analyses. Newly generated sequences are set in **bold**

Classification	Source	Accession numbers					
		nr18S	nr28S	*rpb1*	*rpb2*	5.8S	*tef1*
Agaricomycetes / Agaricales							
Asterophora lycoperdoides	CBS 170.86	AF223190	DQ367417	EF421021	DQ367431	AF357037	DQ367424
Coprinus comatus	AFTOL-ID 626	AY635772	AY665772	AY857983	AY780934	AY854066	—
Gymnopilus picreus	ZRL2015011	KY418882	KY418948	KY418980	KY419027	LT716066	KY419077
Gymnopus confluens	ZRL20151148	KY418870	KY418936	—	KY419016	LT716054	KY419070
Hydropus marginellus	AFTOL-ID 1720	DQ457674	DQ444856	—	DQ472722	DQ490627	—
Lepiota cristata	ZRL20151133	KY418841	KY418910	—	KY418992	LT716026	KY419048
Marasmius oreades	ZRL2015086	KY418864	KY418930	KY418972	KY419010	LT716048	KY419066
Psathyrella candolleana	ZRL20151400	KY418879	KY418945	KY418978	KY419024	LT716063	KY419075
Agaricomycetes / Amylocorticiales							
Amylocorticium cebennense	HHB-2808	GU187561	GU187612	GU187439	GU187770	GU187505	GU187675
Anomoloma myceliosum	MJL-4413	GU187559	GU187614	GU187441	GU187766	GU187500	GU187677
Podoserpula ailaoshanensis	ZJL2015015	KU324487	KU324491	—	—	KU324484	KU324494
Podoserpula pusio	AFTOL-ID 1522	DQ470821	—	—	—	DQ494688	—
Agaricomycetes / Atheliales							
Athelia arachnoidea	CBS 418.72	GU187557	GU187616	GU187436	GU187769	GU187504	GU187672
Leptosporomyces raunkiaerii	HHB-7628	GU187588	GU187640	GU187471	GU187791	GU187528	—
Piloderma fallax	S-12	GU187591	GU187644	—	GU187797	GU187535	GU187738
Agaricomycetes / Auriculariales							
Auricularia heimuer	Xiaoheimao	KY418890	—	—	KY419035	LT716074	KY419083
Exidia sp.	PBM2527	AY700191	—	—	—	DQ241774	DQ408144
Agaricomycetes / Boletales							
Coniophora arida	FP104367	GU187573	GU187622	GU187445	GU187775	GU187510	GU187684
Gomphidius roseus	MB 95-038	DQ534669	DQ534682	GU187459	GU187818	DQ534570	GU187702
Gyrodontium sacchari	MUCL40589	GU187579	GU187632	GU187460	GU187764	GU187522	GU187703
Leucogyrophana lichenicola	DAOM194172	GU187583	GU187638	GU187467	GU187789	GU187531	GU187715
Serpula lacrymans	REG-383	GU187596	GU187649	GU187485	GU187809	GU187542	GU187752
Suillus pictus	MB03-093	AY684154	—	AY858965	AY786066	AY854069	AY883429
Agaricomycetes / Cantharellales							
Botryobasidium botryosum	AFTOL-ID 604	DQ089013	AY662667	—	—	DQ267124	—
Hydnum repandum	BB 07.341	KF294643	—	—	KF294720	—	JX192980
Multiclavula mucida	AFTOL-ID 1130	AY885163	—	—	—	DQ521417	—
Agaricomycetes / Corticiales							
Corticium roseum	MG46	AY463401	—	—	—	GU590877	—
Dendrothele maculata	—	AY586652	—	—	—	AY463404	—
Punctularia strigosozonata	AFTOL-ID 1248	AF518642	AF518586	DQ831031	DQ381843	DQ398958	DQ408147
Agaricomycetes / Geastrales							
Geastrum recolligens	OSC41996	DQ218486	—	—	DQ219052	—	DQ219230
Pyrenogaster pityophilus	OSC59743	DQ218519	—	—	DQ219057	—	DQ219232
Agaricomycetes / Gloeophyllales							
Boreostereum radiatum	RLG-9717-sp	HM536050	HM536051	—	HM536101	HM536085	—
Chaetodermella luna	NH 8482	EU118615	—	—	—	—	—
Gloeophyllum sepiarium	Wilcox-3BB	HM536061	HM536062	—	—	HM536091	HM536110
Gloeophyllum striatum	ARIZAN027866	HM536063	HM536064	—	—	HM536092	—
Gloeophyllum subferrugineum	FPRI-508	HM536065	HM536066	—	—	—	—
Gloeophyllum trabeum	1320	HM536067	HM536068	—	HM536112	HM536094	HM536113
Griseoporia carbonaria	FP-97972-Sp	HM536054	HM536055	—	HM536104	—	HM536105

© 2020 Westerdijk Fungal Biodiversity Institute

Table 1. (Continued).

Classification	Source	Accession numbers					
		nr18S	nr28S	*rpb1*	*rpb2*	5.8S	*tef1*
Griseoporia taiwanense	Dai 11560	KC782730	—	—	—	JX524624	—
Heliocybe sulcata	IBUG-9930	HM536069	HM536070	—	HM536114	HM536095	HM536115
Hispidaedalea imponens	He 1546	KC782742	—	—	—	KC345726	—
Jaapia argillacea	CBS 252.74	GU187581	AF518581	GU187463	GU187788	GU187524	GU187711
Jaapia ochroleuca	MA-Fungi 23942	—	—	—	—	LN824166	—
Neolentinus adhaerens	DAOM214911	—	HM536072	—	—	HM536096	HM536117
Neolentinus kauffmanii	DAOM214904	HM536073	HM536074	—	—	HM536097	HM536118
Neolentinus lepideus	DAOM208724	HM536077	HM536078	—	HM536121	—	HM536122
Osmoporus mexicanum	FP-104133-Sp	HM536056	HM536057	—	—	HM536088	HM536106
Osmoporus odoratus	Wu 0309-92	EF153195	—	—	—	—	—
Osmoporus protractum	H-80	HM536059	HM536060	—	HM536107	HM536090	HM536108
Paratrichaptum accuratum	**GC 1708-180**	**LC473734**	**LC473736**	**LC473738**	**LC473740**	**LC473732**	**LC473742**
Paratrichaptum accuratum	**GC 1708-183**	**LC473735**	**LC473737**	**LC473739**	**LC473741**	**LC473733**	**LC473743**
Veluticeps abietina	GBB-398	HM536079	HM536080	—	HM536123	—	HM536124
Veluticeps berkeleyi	HHB-8594	HM536081	HM536082	—	HM536125	HM536099	—
Veluticeps fimbriata	L-10628	HM536083	HM536084	—	HM640260	HM536100	HM536127
Agaricomycetes / Gomphales							
Clavariadelphus truncatus	OSC67280	AY574649	—	—	DQ219064	—	DQ219240
Phaeoclavulina grandis	OSC122773	DQ218618	—	—	DQ219074	—	DQ219252
Agaricomycetes / Hymenochaetales							
Alloclavaria purpurea	AFTOL-ID 1736	DQ457657	DQ437679	—	—	—	—
Oxyporus corticola	ZRL20151459	KY418899	KY418954	—	KY419038	LT716075	KY419087
Peniophorella praetermissa	AFTOL-ID 518	AY700185	AY707094	—	AY787221	AY854081	—
Tropicoporus linteus	MUCL47139	GU462002	—	—	—	GU461973	GU461936
Agaricomycetes / Hysterangiales							
Aroramyces gelatinosporus	H4010	DQ218524	—	—	DQ218941	—	DQ219118
Chondrogaster pachysporus	OSC49298	DQ218538	—	—	DQ218958	—	DQ219136
Agaricomycetes / Lepidostromatales							
Ertzia akagerae	BR	FJ171733	—	—	—	—	—
Lepidostroma calocerum	R05	FJ171737	—	—	—	—	—
Sulzbacheromyces caatingae	DNA5385	KC170318	—	—	—	—	—
Agaricomycetes / Phallales							
Dictyophora duplicata	OSC38819	DQ218481	—	—	DQ219087	—	DQ219265
Phallus costatus	MB02040	DQ218513	—	—	DQ219104	—	DQ219279
Agaricomycetes / Polyporales							
Antrodia serialis	KHL12010	JX109844	—	—	JX109870	JX109844	—
Bjerkandera adusta	HHB 12826	KP135198	—	KP134784	KP134913	KP134983	—
Climacodon septentrionalis	ZW	AY684165	AY705964	AY864872	AY780941	AY854082	AY885151
Daedalea quercina	FP-56429	KY948883	—	KY948989	—	KY948809	—
Fomitopsis pinicola	AFTOL-770	AY684164	AY705967	AY864874	AY786056	AY854083	AY885152
Ganoderma australe	ZRL20151500	KY418900	KY418955	—	—	LT716076	KY419088
Grifola frondosa	DSH s.n.	AY629318	AY705960	AY864876	AY786057	AY854084	AY885153
Irpex lacteus	DO 421/951208	JX109852	—	—	JX109882	JX109852	—
Lentinus strigosus	ZRL20151738	KY418901	KY418956	—	KY419039	LT716077	KY419089
Phanerochaete chrysosporium	FPL5175	AF287883	AF026593	AY864880	—	AY854086	AY885155
Postia lactea	Kotiranta 20058	KC595939	—	KY948979	—	KC595939	—
Trametes sanguinea	ZRL2015009	KY418902	KY418957	KY418983	KY419040	LT716078	KY419090

© 2020 Westerdijk Fungal Biodiversity Institute

Table 1. (Continued).

Classification	Source	Accession numbers					
		nr18S	nr28S	*rpb1*	*rpb2*	5.8S	*tef1*
Trametes versicolor	ZRL20151477	KY418903	KY418958	—	KY419041	LT716079	KY419091
Agaricomycetes / Russulales							
Bondarzewia montana	AFTOL-ID 452	DQ234539	—	DQ256049	AY218474	DQ200923	DQ059044
Hericium americanum	AFTOL-ID 469	DQ411538	—	—	—	DQ206987	DQ028585
Heterobasidion annosum	AFTOL-ID 470	—	—	DQ667160	AH013701	DQ206988	DQ028584
Lactifluus deceptivus	AFTOL-ID 682	AY631899	AY707093	—	AY803749	AY854089	AY885158
Agaricomycetes / Sebacinales							
Craterocolla cerasi	TUB020203	KF061265	—	—	KF061300	KF061265	—
Tremellodendron pallidum	AFTOL-ID 699	—	AY766081	—	DQ408132	DQ411526	DQ029196
Agaricomycetes / Stereopsidales							
Stereopsis radicans	OLR45395	KC203496	KC203496	—	KC203502	—	KC203516
Stereopsis sp.	OKHL15544	—	KC203499	—	KC203505	—	KC203519
Agaricomycetes / Thelephorales							
Boletopsis leucomelaena	PBM2678	DQ154112	DQ435797	GU187494	GU187820	DQ484064	GU187763
Thelephora ganbajun	ZRL20151295	KY418908	KY418962	KY418987	KY419043	LT716082	KY419093
Tomentella sp.	AFTOL-ID 1016	DQ835997	DQ092920	—	DQ835999	DQ835998	—
Agaricomycetes / Trechisporales							
Subulicystidium sp.	KHL10780	AY586714	—	—	—	AY463468	—
Trechispora alnicola	AFTOL-ID 665	AY635768	AY657012	—	—	DQ411529	DQ059052
Dacrymycetes							
Dacryopinax spathularia	AFTOL-ID 454	AY701525	AY771603	AY857981	—	AY854070	AY881020
Calocera cornea	AFTOL-ID 438	AY701526	AY771610	AY857980	AY536286	AY789083	AY881019
Tremellomycetes							
Bullera alba	CBS 501	AF075500	X60179	KF036334	KF036745	AF444368	KF037016
Dioszegia antarctica	CBS 10920	FJ640575	KF036667	KF036444	KF036858	DQ402529	KF037129

Taxonomy

Gloeophyllales Thorn, *Mycol. Res*. **111**: 540. 2007.
Synonym: *Jaapiales* Manfr. Binder, K.H. Larss. & Hibbett, *Mycologia* **102**: 871. 2010

Type genus: *Gloeophyllum*.

Notes: *Jaapiales* is placed here in synonymy with *Gloeophyllales* based on our phylogram (Fig. 1). *Gloeophyllales*, including a single family *Gloeophyllaceae*, mostly accommodates polypore genera (*e.g.*, *Gloeophyllum*, *Griseoporia*, *Heliocybe*, *Hispidaedalea*, *Paratrichaptum*, *Neolentinus*, and *Osmoporus*), and some agaricoid (*e.g.*, *Heliocybe* and *Neolentinus*) and corticoid genera (*e.g.*, *Boreostereum*, *Chaetodermella*, *Jaapia*, and *Veluticeps*).

The concept of *Gloeophyllales* is in agreement with Hibbett *et al.* (2007) but expanded to encompass the genus *Jaapia* with pigmented, narrowly fusoid, and cyanophilous basidiospores. Almost all genera in *Gloeophyllales* cause brown rot, except for *Boreostereum* and *Jaapia* for which rot type remains unclear. *Boreostereum* is possibly associated with white rot (Martin & Gilbertson 1980) but also viewed as brown rot (Chamuris 1988); *Jaapia* may belong to a new type of brown rot based on genomic analyses (Riley *et al.* 2014).

Gloeophyllaceae Jülich, *Bibl. Mycol.* **85**: 368. 1981.
Synonyms: *Boreostereaceae* Jülich, *Bibl. Mycol.* **85**: 357. 1981. *Jaapiaceae* Manfr. Binder, K.H. Larss. & Hibbett, *Mycologia* **102**: 871. 2010.

Type genus: *Gloeophyllum*.

Note: The names *Boreostereaceae* and *Jaapiaceae* are considered here as synonyms of *Gloeophyllaceae* based on our phylogram (Fig. 1).

Paratrichaptum Corner, *Nova Hedwigia, Beih*. **86**: 136. 1987.

Type species: *Paratrichaptum accuratum*.

Basidiocarps pileate, sessile. Pilei yellowish brown to dark brown, applanate to triquetrous. Pore surface grey to pale purplish grey when fresh, turning to brown to blackish brown when dry; pores angular to daedaleoid, with thick dissepiments. Hyphal system monomitic in both context and trama. All hyphae nodose-septate, branching from the clamp. Context hyphae yellowish brown, thick-walled. *Tramal hyphae* yellowish brown, thick-walled. *Cystidia* fasciculate, thick-walled. *Basidia* subclavate to clavate, pale yellowish brown, thin- to slightly thick-walled, with two to four sterigmata. *Basidiospores* broadly ellipsoid

© 2020 Westerdijk Fungal Biodiversity Institute

to ellipsoid, pale brown, thin- to slightly thick-walled, smooth, inamyloid, non-dextrinoid, acyanophilous.

Paratrichaptum accuratum Corner, *Nova Hedwigia, Beih*. **86**: 136. 1987. Figs 2, 3.

Typus: **Indonesia**, Sumatra, Brastagi, alt. 2 000 m, on a dead fallen trunk in montane forest, 15 Sep. 1931, *E.J.H. Corner*, holotype (E?).

Basidiocarps probably perennial, broadly sessile, pileate, solitary, soft-corky and spongy when fresh, corky and light in weight when dry, without odour, temporarily becoming black in KOH in all parts of the fruiting body. Pilei applanate to triquetrous, semicircular, projecting up to 14 cm, up to 28 cm wide and up to 15 cm thick at base. Pileal surface yellowish brown to dark brown, glabrous to velutinous, covered by mosses in old specimens; margin obtuse when young, sharper with age. Pore surface grey to pale purplish grey when fresh, turning to brown to blackish brown when dry; pores angular to irregular when young, becoming daedaleoid with age, 0.5–1.5 per mm, dissepiments thick, entire and sterile; single pores up to 1 cm long and 2 mm wide when daedaleoid. Tubes brown, corky, up to 1.5 cm deep, tube layers distinct, new layer successively grow from the dead ones. Context, dark brown, corky, fibrous, up to 6 cm thick, homogeneous. Hyphal system monomitic in both context and trama. All hyphae nodose-septate, branching from the clamp. Context hyphae yellowish brown, fairly straight, occasionally branched, 5–7.5 µm diam, with 0.5–1 µm diam thick walls, loosely interwoven. *Tramal hyphae* yellowish brown, fairly straight, occasionally branched, 2.5–5.5 µm diam, with 0.5–1 µm diam thick walls, loosely interwoven. *Cystidia* cylindrical to subclavate, with obtuse apex, straight to slightly flexuous, fasciculate, projecting, pale brown to yellowish brown, 30–90 × 3–6 µm, with 0.5–1 µm diam thick walls. *Basidia* subclavate to clavate, usually with four sterigmata, rarely with two or three sterigmata, pale brown, thin- to slightly thick-walled, with 0.2–0.4 µm diam walls, 20–34 × 4–5.5 µm. *Basidiospores* broadly ellipsoid to ellipsoid, pale brown, thin- to slightly thick-walled, with 0.2–0.4 µm thick walls, smooth, sometimes with small oil-drops, inamyloid, non-dextrinoid, acyanophilous, mostly 3.4–4.9 × 2.4–3.2 µm. (3.1–)3.4–4.4(–5.2) × (2.1–)2.4–3(–3.5) µm, L = 3.9 ± 0.5 µm, W = 2.7 ± 0.3 µm, Q = 1.45 (n = 30) (GC 1708-180); (3.2–)3.6–4.6(–5.1) × (2.2–)2.4–2.9 (–3.3) µm, L = 4.1 ± 0.5 µm, W = 2.7 ± 0.3 µm, Q = 1.54 (n = 30) (GC 1708-183); (3.5–)4–4.9 (–5.3) × (2.4–)2.6–3.2(–3.6) µm, L = 4.4 ± 0.4 µm, W = 2.9 ± 0.3 µm, Q = 1.53 (n = 30) (TFM F-17203).

Distribution: Asian species. First described from a highland forest in Indonesia (Sumatra) (Corner 1987), later reported from subtropical to boreal regions of Japan (Hokkaido, Kagoshima, Nara, Yamagata), Taiwan (Núñez & Ryvarden 2001, Hattori 2017), and China (Yunnan, this study).

Ecology: On dead or living angiosperm trunks in old-growth forest, occurring in August to October (Corner 1987, Hattori 2017).

Type of rot: Brown rot (Hattori 2017).

Specimens examined: **China**, Yunnan Province, Wenshan Zhuang and Miao Autonomous Prefecture, Maguan County, Gulinjing Township, 22°51'33" N 104°00'25" E, alt. 1 772 m, on living angiosperm trunk, 9 Aug. 2017, *C.C. Chen*, GC 1708-183 (TNM F32585); 22°51'34"N 103°59'36"E, alt. 1 895 m, on living angiosperm trunk in a subtropical evergreen broad-leaved forest dominated by *Alcimandra*, *Lithocarpus* and *Manglietia*, 9 Aug. 2017, *C.C. Chen*, GC 1708-180 (KUN HKAS104962 & TNM F32584). **Japan**, Nara Prefecture, Mt. Wasamata, 30 Aug. 1994, *N. Iwata* (TFM F-17203). **Taiwan**, 25 Sep. 1922, *R. Kanehira* (miswritten as *A. Kanehira* on specimen label, Fig. 2H) (O-F-911778).

Notes: *Paratrichaptum accuratum* was described based on a single specimen (Corner 1987). Hattori (2001), as well as this study, failed to trace the holotype or other original material of *P. accuratum* deposited in the herbarium of Royal Botanic Garden Edinburgh (E). Instead, we studied some specimens from China, Japan, and Taiwan. The peculiar combination of morphological features makes *P. accuratum* easy to identify. Our studied specimens correspond well with Corner's (1987) descriptions and illustrations for this species, although some minor differences were noticed. First, the basidiocarp tissue of *P. accuratum* temporarily turns black in KOH, which was not mentioned in the protologue. Second, the species was reported as annual (Corner 1987). However, one of our specimens (GC 1708-180) developed a new tube layer successively growing from old ones (Fig. 2B–E). Third, we found some mature basidiospores of *P. accuratum* that are of a slightly darker colour and with thicker walls (Fig. 3E).

A Taiwanese specimen of *P. accuratum* (O-F-911778), collected on 25 September 1922 by the Japanese botanist R. Kanehira, lacks detailed location information (Fig. 2H). However, we presume it is likely collected from montane areas near to Lala Mountain, Taoyuan, because he made a field trip to Lala Mountain during the same period according to plant specimen records retrieved from the online database of TAIF (http://taif.tfri.gov.tw/search.php). Lala Mountain area lies in the warm temperate region, within the native range of *P. accuratum*.

DISCUSSION

The present study places *Paratrichaptum* in the family *Gloeophyllaceae* (*Gloeophyllales, Agaricomycetes*) based on studies derived from morphological features and phylogenetic analyses of sequences of six genes (Figs 1–3). Our study also shows that a corticoid genus *Jaapia* with two species (*viz.*, *J. argillacea* and *J. ochroleuca*) is classified in *Gloeophyllaceae* and *Gloeophyllales* according to phylogenetic evidence (Fig. 1), although *Jaapia* was placed in the family *Jaapiaceae* and the order *Jaapiales* by Binder *et al*. (2010). As a result, *Jaapiaceae* and *Jaapiales* become synonyms of *Gloeophyllaceae* and *Gloeophyllales*, respectively.

Regarding the family-level classification of *Gloeophyllales*, we unite all taxa in a single family (*viz.*, *Gloeophyllaceae*) because the resolution of the six-gene phylogeny and taxon sampling are not enough to resolve the family relationships at the moment. Nevertheless, the possibility to recover the families *Boreostereaceae* and *Jaapiaceae*, or even to introduce a new family for *Paratrichaptum* cannot be excluded when data from whole-genome studies become available.

The topology of our six-gene phylogram (Fig. 1) is consistent with previous studies (Binder *et al*. 2010, Garcia-Sandoval *et al*. 2011, Floudas *et al*. 2012, Hodkinson *et al*. 2014, Sjökvist *et al*. 2014, Nagy *et al.* 2015, Garnica *et al*. 2016, Zhao *et al*.

© 2020 Westerdijk Fungal Biodiversity Institute

Fig. 2. *Paratrichaptum accuratum*. **A.** Native habitat of GC 1708-180 at Maguan County, Yunnan, China, 9 August 2017. **B–C.** Basidiocarp on living angiosperm trunk (GC 1708-180). **D.** Pore surface *in situ* (GC 1708-180). **E.** Partial dried specimen of GC 1708-180. **F–G.** Dried specimen of GC 1708-183. **H–I.** Dried specimen of O-F-911778 (photographed by Katriina Bendiksen). This specimen seems to be a duplicate from the herbarium of Government Forest Experiment Station, Tokyo, Japan. It is noted that the correct name for the collector is R. Kanehira, a Japanese botanist. Bars: B–C = 5 cm; D = 4 mm; E = 2 cm; F–G, I = 1 cm.

© 2020 Westerdijk Fungal Biodiversity Institute

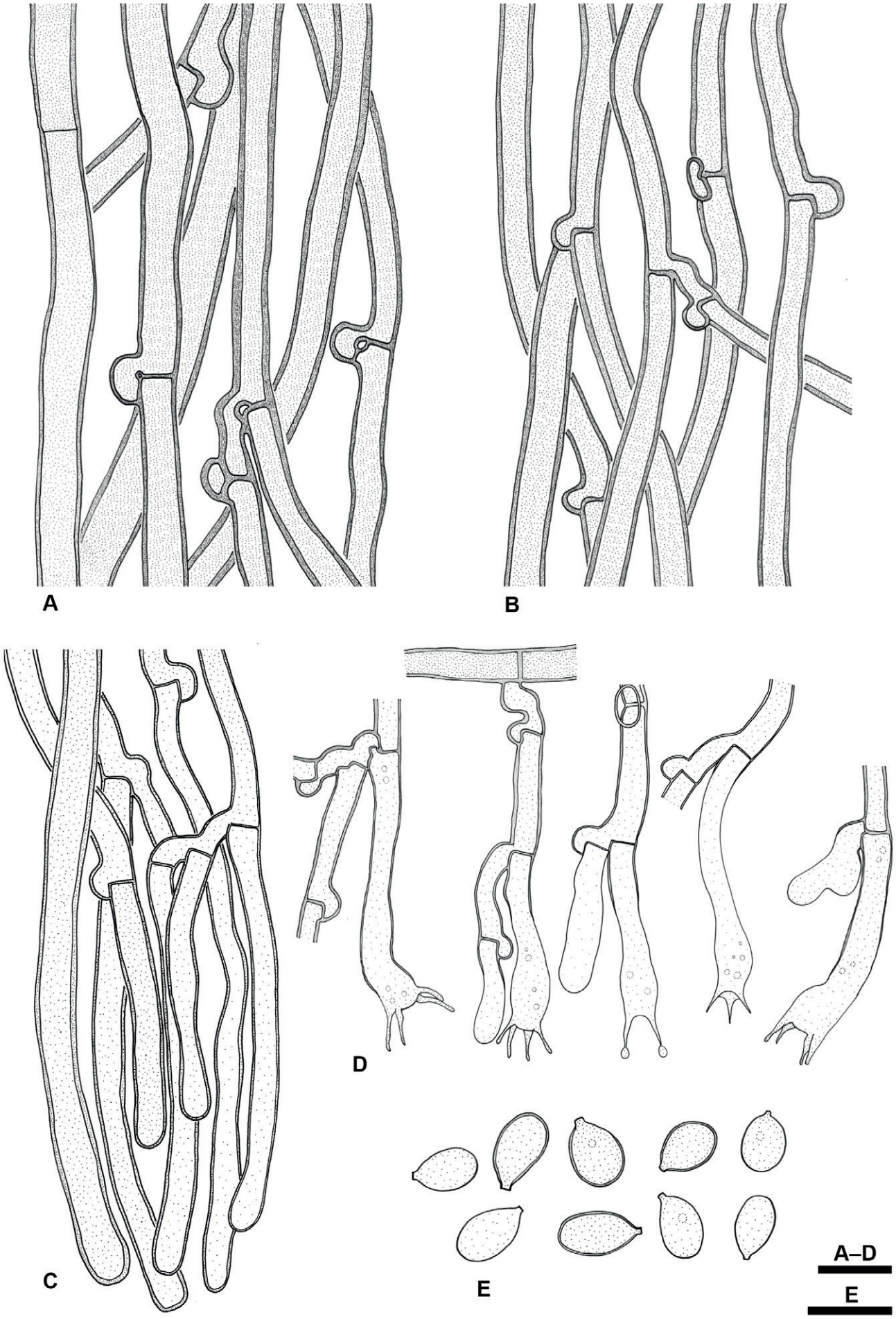

Fig. 3. Microscopic structures of *Paratrichaptum accuratum* (GC 1708-183). **A, B.** Hyphae from context. **C.** Cystidia. **D.** Basidia. **E.** Basidiospores. Bars: A–D = 10 µm; E = 5 µm.

© 2020 Westerdijk Fungal Biodiversity Institute

2017). However, deviating taxon- or gene-sampling applied to different analyses may result in different positions of the taxa on trees. For example, a six-gene phylogeny placed *Boreostereum radiatum* as the sister group to the core group of *Gloeophyllales*, consisting of the genera *Chaetodermella*, *Gloeophyllum*, *Heliocybe*, *Neolentinus*, *Osmoporus*, and *Veluticeps* (Garcia-Sandoval *et al*. 2011). In our analysis, *B. radiatum* is recovered as a sister taxon to *Paratrichaptum accuratum*, but the position is weakly supported. Another six-gene phylogeny placed *Jaapia* as the sister group to *Agaricomycetidae*, consisting of *Agaricales*, *Amylocorticiales*, *Atheliales*, and *Boletales* (Binder *et al*. 2010), whereas in our analysis *Jaapia* is placed in *Gloeophyllales*.

Paratrichaptum represents the earliest diverging lineage in *Gloeophyllales*, yielding a new picture of this order. For example, with the addition of *Paratrichaptum*, pileate basidiocarps and brown rot appear to be ancestral states of *Gloeophyllales*. Besides, brown rot could be synapomorphic in *Gloeophyllales*, although the rot type of *Boreostereum* and *Jaapia* should be further confirmed. Moreover, genera from the basal lineages of *Gloeophyllales* (*Boreostereum*, *Jaapia*, and *Paratrichaptatum*) possess pigmented basidiospores, while the rest of the members of *Gloeophyllales* possess colorless basidiospores. Like most members of *Gloeophyllales*, *Paratrichaptum* has brownish context but lacks dimitic to trimitic hyphal system, and posesses clamp connections. There is no morphological synapomorphy to unite *Gloeophyllales*.

Paratrichaptum accuratum may represent a relic species, according to its phylogenetic position, peculiar distribution pattern and rare occurrence. On the phylogram (Fig. 1), *P. accuratum* does not have any close relatives and has relatively long genetic distances from other members in *Gloeophyllales*. Very few collections of *P. accuratum* were made since 1922. According to available collection information, *P. accuratum* occurs in old-growth subtropical-boreal forests in some disjunct mountain areas of eastern and south-eastern Asia. *Paratrichaptum accuratum* is a threatened species and its conservation status should be assessed based on the criteria in Dahlberg & Mueller (2011). *Paratrichaptum accuratum* grows on dead or living angiosperms, which implies that it presumably colonises living trees and continues to degrade wood after the tree dies.

ACKNOWLEDGEMENTS

This study was financed by the Ministry of Science and Technology of ROC (Taiwan) (Grant no 107-2621-B-178-002-MY3). We are grateful for the help of Dr Xiang-Hua Wang, the mycologist of KUN, who arranged the field trip for the first author to Yunnan, China in Aug 2017 and also aided in phylogenetic analyses. We are indebted to Drs Karl-Henrik Larsson and Katriina Bendiksen (O) for kindly providing Taiwanese specimen photographs, Chiung-Chih Chang (TNM) for adjusting figures, Siou-Zhen Chen (TNM) for curating studied specimens, and Ronnie Gicana (NCHU) for improving the manuscript. We also thank the reviewers and editor for their valuable suggestions and discussions.

REFERENCES

Binder M, Larsson KH, Matheny PB, *et al*. (2010). *Amylocorticiales ord. nov.* and *Jaapiales ord. nov.*: early diverging clades of *Agaricomycetidae* dominated by corticioid forms. *Mycologia* **102**: 865–880.

Chamuris G (1988). The non-stipitate stereoid fungi in the northeastern United States and adjacent Canada. *Mycologia Memoir* **14**: 41–45.

Chen CC, Wu SH, Chen CY (2018). *Hydnophanerochaete* and *Odontoefibula*, two new genera of phanerochaetoid fungi (*Polyporales*, *Basidiomycota*) from East Asia. *MycoKeys* **39**: 75–96.

Corner EJH (1987). Ad Polyporaceas IV. The genera *Daedalea*, *Flabellophora*, *Flavodon*, *Gloeophyllum*, *Heteroporus*, *Irpex*, *Lenzites*, *Microporellus*, *Nigrofomes*, *Nigroporus*, *Oxyporus*, *Paratrichaptum*, *Rigidoporus*, *Scenidium*, *Trichaptum*, *Vanderbylia*, and *Steccherinum*. *Beihefte zur Nova Hedwigia* **86**: 1–265.

Dahlberg A, Mueller GM (2011). Applying IUCN red-listing criteria for assessing and reporting on the conservation status of fungal species. *Fungal Ecology* **4**: 147–162.

Darriba D, Taboada GL, Doallo R, *et al*. (2012). jModelTest 2: more models, new heuristics and parallel computing. *Nature Methods* **9**: 772–772.

Drummond AJ, Suchard MA, Xie D, *et al*. (2012). Bayesian phylogenetics with BEAUti and the BEAST 1.7. *Molecular Biology and Evolution* **29**: 1969–1973.

Floudas D, Binder M, Riley R, *et al*. (2012). The Paleozoic origin of enzymatic lignin decomposition reconstructed from 31 fungal genomes. *Science* **336**: 1715–1719.

Frøslev T, Matheny PB, Hibbett DS (2005). Lower level relationships in the mushroom genus *Cortinarius* (*Basidiomycota*, *Agaricales*): a comparison of *RPB1, RPB2*, and ITS phylogenies. *Molecular Biology and Evolution* **37**: 602–618.

Garcia-Sandoval R, Wang Z, Binder M, *et al*. (2011). Molecular phylogenetics of the *Gloeophyllales* and relative ages of clades of *Agaricomycotina* producing a brown rot. *Mycologia* **103**: 510–524.

Garnica S, Riess K, Schön ME, *et al*. (2016). Divergence times and phylogenetic patterns of *Sebacinales*, a highly diverse and widespread fungal lineage. *PLoS One* **11**: e0149531.

Hall TA (1999). BioEdit: A user-friendly biological sequence alignment editor and analysis program for Windows 95/98/NT. *Nucleic Acids Symposium Series* **41**: 95–98.

Hattori T (2001). Type studies of the polypores described by EJH Corner from Asia and West Pacific areas II. Species described in *Gloeophyllum*, *Heteroporus*, *Microporellus*, *Oxyporus*, *Paratrichaptum*, and *Rigidoporus*. *Mycoscience* **42**: 19–28.

Hattori T (2017). Biogeography of polypores in Malesia, Southeast Asia. *Mycoscience* **58**: 1–13.

He SH, Vlasák J, Dai YC (2014). *Hispidaedalea gen. nov.* and *Griseoporia taiwanense sp. nov.* (*Gloeophyllales*, *Basidiomycota*) based on morphological and molecular characters. *Mycological Progress* **13**: 833–839.

Hibbett DS, Binder M, Bischoff JF, *et al*. (2007). A higher-level phylogenetic classification of the Fungi. *Mycological Research* **111**: 509–547.

Hillis DM, Bull JJ (1993). An empirical test of bootstrapping as a method for assessing confidence in phylogenetic analysis. *Systematic Biology* **42**: 182–192.

Hodkinson BP, Moncada B, Lücking R (2014). *Lepidostromatales*, a new order of lichenized fungi (*Basidiomycota*, *Agaricomycetes*), with two new genera, *Ertzia* and *Sulzbacheromyces*, and one new species, *Lepidostroma winklerianum*. *Fungal Diversity* **64**: 165–179.

Katoh K, Standley DM (2013). MAFFT multiple sequence alignment software version 7: improvements in performance and usability. *Molecular Biology and Evolution* **30**: 772–780.

Kumar S, Stecher G, Tamura K (2016). MEGA7: molecular evolutionary genetics analysis version 7.0 for bigger datasets. *Molecular Biology and Evolution* **33**: 1870–1874.

© 2020 Westerdijk Fungal Biodiversity Institute

Liu YJ, Whelen S, Hall BD (1999). Phylogenetic relationships among ascomycetes: evidence from an RNA polymerse II subunit. *Molecular Biology and Evolution* **16**: 1799–1808.

Lutzoni F, Kauff F, Cox CJ, *et al*. (2004). Assembling the fungal tree of life: progress, classification, and evolution of subcellular traits. *American Journal of Botany* **91**: 1446–1480.

Martin K, Gilbertson R (1980). Synopsis of wood-rotting fungi on spruce in North America: III. *Mycotaxon* **10**: 479–501.

Matheny PB (2005). Improving phylogenetic inference of mushrooms with RPB1 and RPB2 nucleotide sequences (*Inocybe*; *Agaricales*). *Molecular Phylogenetics and Evolution* **35**: 1–20.

Matheny PB, Wang Z, Binder M, *et al*. (2007). Contributions of *rpb2* and *tef1* to the phylogeny of mushrooms and allies (*Basidiomycota*, *Fungi*). *Molecular Phylogenetics and Evolution* **43**: 430–451.

Miller MA, Pfeiffer W, Schwartz T (2010) Creating the CIPRES Science Gateway for inference of large phylogenetic trees. Proceeding of the Gateway Computing Environments Workshop (GCE). 14 November 2010. Los Angeles, USA: 1–8.

Moncalvo JM, Lutzoni FM, Rehner SA, *et al*. (2000). Phylogenetic relationships of agaric fungi based on nuclear large subunit ribosomal DNA sequences. *Systematic Biology* **49**: 278–305.

Nagy LG, Riley R, Tritt A, *et al*. (2015). Comparative genomics of early-diverging mushroom-forming fungi provides insights into the origins of lignocellulose decay capabilities. *Molecular Biology and Evolution* **33**: 959–970.

Núñez M, Ryvarden L (2001). East Asian polypores 2. *Polyporaceae s. lato*. *Synopsis Fungorum* **14**: 170–522.

Rambaut A, Drummond AJ, Xie D, *et al*. (2018). Posterior summarization in Bayesian phylogenetics using Tracer 1.7. *Systematic Biology* **67**: 901–904.

Rehner SA, Buckley E (2005). A *Beauveria* phylogeny inferred from nuclear ITS and *EF1-α* sequences: evidence for cryptic diversification and links to *Cordyceps* teleomorphs. *Mycologia* **97**: 84–98.

Riley R, Salamov AA, Brown DW, *et al*. (2014). Extensive sampling of basidiomycete genomes demonstrates inadequacy of the white-rot/brown-rot paradigm for wood decay fungi. *Proceedings of the National Academy of Sciences* **111**: 9923–9928.

Robert V, Stegehuis G, Stalpers J (2005). The MycoBank engine and related databases. 16 September 2019. http://www.mycobank.org.

Ronquist F, Teslenko M, Van der Mark P, *et al*. (2012). MrBayes 3.2: efficient Bayesian phylogenetic inference and model choice across a large model space. *Systematic Biology* **61**: 539–542.

Ryvarden L (1991). Genera of polypores: nomenclature and taxonomy. *Synopsis Fungorum* **5**: 1–363.

Sánchez-Ramírez S, Tulloss RE, Amalfi M, *et al*. (2015). Palaeotropical origins, boreotropical distribution and increased rates of diversification in a clade of edible ectomycorrhizal mushrooms (*Amanita* section *Caesareae*). *Journal of Biogeography* **42**: 351–363.

Sela I, Ashkenazy H, Katoh K, *et al*. (2015). GUIDANCE2: accurate detection of unreliable alignment regions accounting for the uncertainty of multiple parameters. *Nucleic Acids Research* **43**: W7–W14.

Sjökvist E, Pfeil BE, Larsson E, *et al*. (2014). *Stereopsidales* - a new order of mushroom-forming fungi. *PLoS One* **9**: e95227.

Stamatakis AJB (2014). RAxML version 8: a tool for phylogenetic analysis and post-analysis of large phylogenies. *Bioinformatics* **30**: 1312–1313.

Stöver BC, Müller KF (2010). TreeGraph 2: Combining and visualizing evidence from different phylogenetic analyses. *BMC Bioinformatics* **11**: 1–9.

Telleria MT, Dueñas M, Melo I, *et al*. (2015). Spelling out *Jaapia* species. *Mycological Progress* **14**: 57.

White TJ, Bruns T, Lee S, *et al*. (1990) Amplification and direct sequencing of fungal ribosomal RNA genes for phylogenetics. In: *PCR protocols: a guide to methods and applications* (Innis MA, Gelfand DH, Sninsky JJ, *et al*., eds). Academic Press, San Diego, USA: 315–322.

Zhao RL, Li GJ, Sánchez-Ramírez S, *et al*. (2017). A six-gene phylogenetic overview of *Basidiomycota* and allied phyla with estimated divergence times of higher taxa and a phyloproteomics perspective. *Fungal Diversity* **84**: 43–74.

© 2020 Westerdijk Fungal Biodiversity Institute